J. Chem. Thermodynamics **1969**, 1, 543–557

Magnetite (Fe_3O_4) Heat capacity and thermodynamic properties from 5 to 350 K, low-temperature transition

EDGAR F. WESTRUM, Jr.

Department of Chemistry, University of Michigan, Ann Arbor Michigan 48104, U.S.A.

and

FREDRIK GRØNVOLD

Chemical Institute A, University of Oslo, Blindern Oslo 3, Norway

(*Received 3 June 1969*)

The heat capacity of synthetic Fe_3O_4 has been measured over the range from 5 to 350 K. Values of thermodynamic functions have been calculated and C_p, $S°$, and $(H°-H_0°)/T$ at 298.15 K are 36.04, 34.93, and 19.85 cal mol^{-1} K^{-1}, respectively. In this sample the previously known λ-type transition was found to consist of two maxima, a larger one at 118.9 K and a smaller one at 113.3 K, with entropy increments of 1.2 cal mol^{-1} K^{-1} and 0.2 cal mol^{-1} K^{-1}, respectively. The mechanism of the transitions is discussed.

1. Introduction

The low-temperature heat capacity of Fe_3O_4 was measured by Parks and Kelley[1] on large natural crystals of magnetite. A marked transition presumably related to changes in the magnetic properties was observed in the temperature interval 113 to 117 K. Millar[2] later determined the heat capacity of magnetite over the range 60 to 300 K on an ore sample containing 99.0 per cent Fe_3O_4 and corrected for 0.67 per cent Fe_2O_3 and 0.37 per cent impurities (largely quartz). A pronounced heat-capacity maximum of 37.1 cal mol^{-1} K^{-1} was found at 114.15 K. The heat-capacity measurements agreed with those of Parks and Kelley at the lowest temperatures, but were about 5.8 per cent lower at 298 K. Calculation of the entropy gave $S(298\ K) = (34.69 \pm 0.2)$ cal mol^{-1} K^{-1} in good agreement with the value 35.1 of Parks and Kelley. The anomalous change in heat capacity around 115 K was observed also by means of differential thermal analysis.[3,4] More recently, the heat capacity was measured in the range 1.8 to 4.2 K on a natural magnetite crystal[5] and on synthetic samples,[6,7] and the spin-wave contribution to the heat capacity was studied.

The fact that the observed peak in the heat capacity occurs about 5 K lower than the abrupt change observed in careful studies of electrical[8] and thermal[9] conductivity suggests the behavior to be significantly dependent upon the composition and

purity of the magnetite and that thermophysical measurements on a sample of unambiguous purity and homogeneity are desiderata. For these reasons measurements were made on synthetically prepared Fe_3O_4. In addition, a sample of magnetite from Kiruna, Sweden, was studied, but it did not show a pronounced heat-capacity anomaly.

2. Experimental

NATURAL MAGNETITE SAMPLE

A sample of natural magnetite from Kiruna, Sweden, was provided from the National Museum collection by Dr. E. C. Robertson of the Geophysics Branch of the United States Geological Survey. It was a cylindrical core, 2.5 cm diameter by 6.2 cm length, diamond drilled from a hand specimen. Chemical and spectrochemical analysis indicated the following composition by mass: 0.23 per cent Si, 0.47 per cent Al, 46.94 per cent Fe^{3+}, 22.58 per cent Fe^{2+}, 0.21 per cent Ca, 0.37 per cent Mg, 1.37 per cent Mn^{2+} and 28.18 per cent O (by association), totalling 100.45 per cent.

The results from the measurements on the Kiruna sample are reported in the supplementary part of this paper,† except for a deviation plot in figure 1.

SYNTHETIC SAMPLE

The synthetic magnetite used in this investigation was prepared from iron(III) oxide and iron. The Fe_2O_3, "Ferrum oxydatum sec. Merck", was heated in an electric furnace at 1000 °C until constant mass was attained. This was achieved after two 4 h heating periods. A small part of the sample was reduced by dry hydrogen gas at 800 °C for 6 h and afterwards crushed to a fine powder. Stoichiometric proportions of this iron and the Fe_2O_3 were heated in an evacuated and sealed silica tube at 1000 °C for 2 days and furnace-cooled.

Quantitative analysis by different investigators gave average values of 72.37 and 72.43 per cent total iron, respectively (theoretical 72.36 per cent) and 24.06 and 24.05 per cent ferrous iron (theoretical 24.12 per cent). Spectrographic analysis showed the presence of about 0.003 per cent Ni and Si, and about 0.001 per cent Cu and Mn.

X-ray powder photographs of the sample showed only lines from Fe_3O_4. Its lattice constant was determined at about 20 °C in an 11.48 cm diameter camera with asymmetric film mounting, using iron radiation [$\lambda(\mathrm{Fe}, K\alpha_1) = 1.93597$ Å]. The value $a = (8.3938 \pm 0.0005)$ Å agrees within the limits of experimental error with that by Tombs and Rooksby[10] and Abrahams and Calhoun,[11] $a = (8.3940 \pm 0.0005)$ Å, and is slightly smaller than that reported by Basta,[12] $a = (8.3963 \pm 0.0005)$ Å. For further results see reference 13.

A specific magnetic moment determination at about 25 °C gave $\sigma = (0.95 \pm 0.02)$ A m^2 g^{-1}. This is in good agreement with the value found by Gorter[14] and is only slightly higher than that found by Weiss and Forrer[15] and Pauthenet.[16]

† Tabulation of the heat capacity of the Kiruna sample has been deposited as NAPS document number 00630 from ASIS National Auxiliary Publications Service, c/o CCM Information Sciences, Inc., 22 West 34th Street, New York, New York 10001. A copy may be secured by citing the document number and remitting $3.00 for photocopies or $1.00 for microfiche in advance by check or money order payable to ASIS–NAPS.

CRYOGENIC TECHNIQUE

The Mark I cryostat and the technique employed for low-temperature adiabatic calorimetry have been described elsewhere.[17] The copper calorimeter (laboratory designation W-9) has a capacity of 90 cm^3; it is gold-plated inside and out and has six vanes. The heat capacity of the empty calorimeter was determined in a separate experiment, using the same amount of indium–tin solder for sealing and Apiezon-T grease for thermal contact between calorimeter, heater, and thermometer. The heat capacity of the calorimeter–heater–thermometer assembly represented from 27 to 75 per cent of the total heat capacity observed (except in the transition region where it decreased to 8 per cent). The platinum resistance thermometer (laboratory designation A-3) has been calibrated by the National Bureau of Standards, and the temperatures are judged to correspond with the thermodynamic temperature scale within 0.1 K from 5 to 10 K, within 0.03 K from 10 to 90 K, and within 0.04 K from 90 to 350 K. Precision is considerably better, and the temperature increments are probably correct to 0.001 K after corrections for quasi-adiabatic drift.

The calorimeter was loaded with sample, and helium was added (after evacuation) to provide thermal contact between sample and calorimeter. The mass of the calorimetric sample was 134.854 g.

3. Results

The heat-capacity determinations are listed in table 1 in chronological order, expressed in terms of the thermochemical calorie equal to 4.184 J. The ice point was taken to be 273.15 K and the relative atomic mass of iron as 55.85. The results are presented in terms of one mole of Fe_3O_4 corresponding to 231.55 g. An analytically-determined curvature correction was applied to the observed values of $\Delta H/\Delta T$. The approximate temperature increments can usually be inferred from the adjacent mean temperatures in table 1.

The heat-capacity *versus* temperature curve is shown in figure 1 and transitions are seen to occur near 116 K. A smaller peak is observed at 113.3 K and a larger one at 118.9 K. Except for the double peak, the results resemble those found earlier by Parks and Kelley[1] and by Millar[2] over the common region (see deviation plot in figure 1).

Values of C_p, $S^\circ - S_0^\circ$, and $(H^\circ - H_0^\circ)/T$ for Fe_3O_4 are listed at selected temperatures in table 2. The Gibbs energy function values are not given because of uncertainty concerning the zero-point entropy of magnetite. The enthalpy and entropy increments were calculated by numerical integration of the heat-capacity values which are considered to have a probable error of about 5 per cent at 5 K, 1 per cent at 10 K, and 0.1 per cent above 25 K. Values below 5 K are extrapolated using the Debye T^3 limiting law. The effects of nuclear spin and isotopic mixing are not included in the entropies. The estimated probable error in the thermodynamic functions is 0.1 per cent above 100 K, but some of the results are given to an additional digit because of their significance on a relative basis.

TABLE 1. Heat capacity of synthetic magnetite (Fe_3O_4)[a]

T/K	C_p/cal mol^{-1} K^{-1}	T/K	C_p/cal mol^{-1} K^{-1}	T/K	C_p/cal mol^{-1} K^{-1}
Series I		101.86	13.473	Series III	
		106.64	14.590		
66.61	6.432	108.15	15.00	112.97	28.34
72.42	7.500	109.64	15.44	113.33	33.2
78.49	8.667	111.08	15.97	113.65	31.5
85.23	10.025	112.41	19.72	114.00	29.7
92.23	11.438	113.46	32.0	114.36	29.0
99.66	12.984	114.38	28.9	114.74	28.4
107.65	14.275	115.35	29.2	115.12	28.5
114.65	28.83	116.29	30.7	115.49	29.6
120.08	32.15	117.16	33.7	115.85	30.4
126.57	18.58	117.95	42.2	116.19	30.7
		118.63	50.2	116.57	28.8
Series II		119.27	47.3	116.99	31.7
		120.02	30.8	117.31	35.1
6.49	0.005 6	121.04	20.1	117.61	38.2
7.67	0.009 9	122.26	18.37	117.90	40.7
8.55	0.015 0	123.54	18.26	118.09	41.4
9.65	0.023 5	125.17	18.14	118.18	43.1
10.56	0.033 6	128.50	18.82	118.27	42.1
11.64	0.049 4	133.01	19.48	118.36	45.5
13.01	0.075 8	139.39	20.42	118.44	46.9
14.33	0.090 4	148.82	21.73	118.53	47.7
15.71	0.114 5	159.81	23.19	118.62	48.2
17.15	0.146 6	170.09	24.48	118.69	42.0
18.68	0.197 4	179.53	25.60	118.77	52.4
20.36	0.261 9	188.38	26.62	118.88	117.0
20.76	0.276 6	197.14	27.57	118.93	52.3
22.87	0.384 3	202.99	28.12	119.01	50.2
24.02	0.454 7	211.81	29.07	119.10	49.8
26.01	0.586 8	220.86	29.95	119.18	48.8
27.98	0.744 4	230.12	30.83	119.26	44.9
30.26	0.950 2	239.24	31.54	119.35	44.8
33.06	1.253	248.52	32.38	119.44	43.3
36.57	1.643	257.89	33.19	119.55	41.7
40.74	2.183	267.11	33.83	119.81	37.1
45.24	2.827	276.17	34.50	120.12	28.6
50.02	3.561	285.24	35.18	120.51	22.84
55.14	4.397	294.51	35.80	120.95	19.98
60.69	5.351	303.96	36.21	121.42	19.15
67.29	6.556	313.44	37.00	121.88	18.62
73.24	7.650	322.91	37.57	122.35	18.24
79.81	8.927	332.59	38.14	122.83	18.22
86.49	10.337	341.64	38.64	123.31	18.02
94.07	11.901	347.94	38.98		

[a] 1 cal = 4.184 J; 1 mol Fe_3O_4 ≙ 231.55 g.

TABLE 2. Thermodynamic properties of synthetic magnetite (Fe_3O_4)[a]

T / K	C_p / cal mol^{-1} K^{-1}	S° / cal mol^{-1} K^{-1}	$(H^\circ - H_0^\circ)/T$ / cal mol^{-1} K^{-1}
10	0.027	0.010	0.006
15	0.101	0.034	0.025
20	0.247	0.080	0.059
25	0.517	0.162	0.122
30	0.928	0.290	0.220
35	1.460	0.472	0.358
40	2.082	0.707	0.534
45	2.789	0.992	0.745
50	3.558	1.326	0.987
60	5.231	2.119	1.553
70	7.045	3.062	2.207
80	8.962	4.126	2.930
90	10.984	5.298	3.712
100	13.063	6.561	4.542
110	15.517	7.912	5.424
120	(32.5)	10.535	7.498
130	19.02	12.065	8.391
140	20.51	13.529	9.203
150	21.89	14.992	10.003
160	23.21	16.447	10.788
170	24.47	17.892	11.556
180	25.66	19.325	12.307
190	26.80	20.743	13.040
200	27.87	22.145	13.755
210	28.90	23.530	14.451
220	29.86	24.897	14.675
230	30.78	26.245	15.791
240	31.66	27.574	16.434
250	32.50	28.884	17.060
260	33.31	30.174	17.670
270	34.08	31.446	18.263
280	34.81	32.699	18.841
290	35.50	33.932	19.404
300	36.16	35.147	19.951
350	39.11	40.948	22.483
273.15	34.31	31.84	18.45
298.15	36.04	34.93	19.85

[a] 1 cal = 4.184 J; 1 mol Fe_3O_4 ≙ 231.55 g.

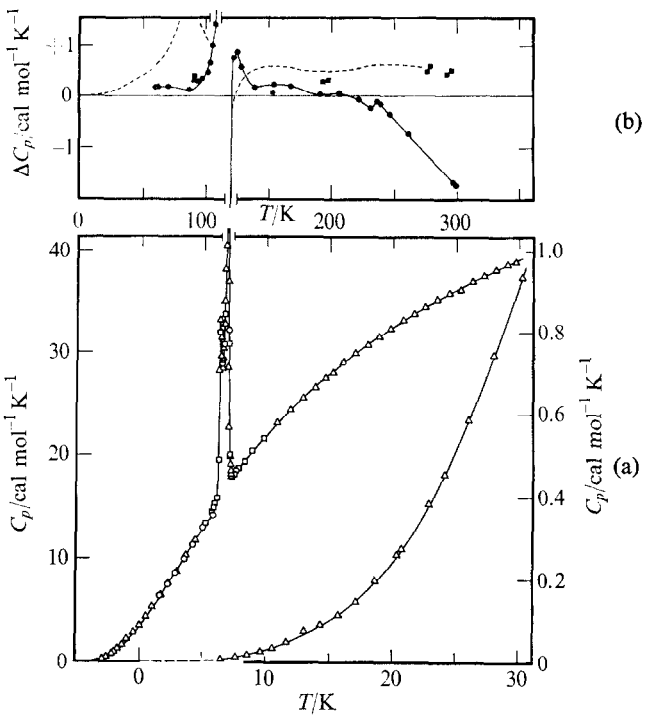

FIGURE 1. (a) Heat capacity of magnetite. ○ represents series I, □ represents series II, △ represents series III. (b) Deviation plot of other measurements from the present ones on synthetic magnetite. ■ represents results of Parks and Kelley,[1] ● represents results of Millar,[2] – – – represents results on Kiruna magnetite.

4. Discussion

GENERAL

The present heat-capacity results are from 0.4 to 3.6 per cent lower than those of Parks and Kelley[1] which accounts for the lower observed entropy at 298.15 K, 34.93 cal mol^{-1} K^{-1} against 35.1 cal mol^{-1} K^{-1}. The results of Millar[2] are about 3 per cent higher at the lowest temperatures, but are about 5 per cent lower at the highest temperatures. His calculated entropy was 34.69 cal mol^{-1} K^{-1}, or slightly lower than the value found here. The enthalpy increments of magnetite above room temperature have most recently been measured by Coughlin *et al.*[18] The derived linear heat-capacity curve crosses the present results at 315 K at only a slight angle; the results are thus in reasonable accord.

An enlarged plot of the heat capacity in the region of low-temperature transition is shown in figure 2. The maximum at 118.88 K is very close to the transition temperature (119.4 K) found by Calhoun,[8] while the lower peak lies close to Millar's[2] transition temperature.

There are no indications of a bifurcated peak in earlier studies.

Several hypotheses can be advanced in explanation of the double peak. For example, only a slight variation of the Fe^{2+}/Fe^{3+} ratio is obviously enough to affect the

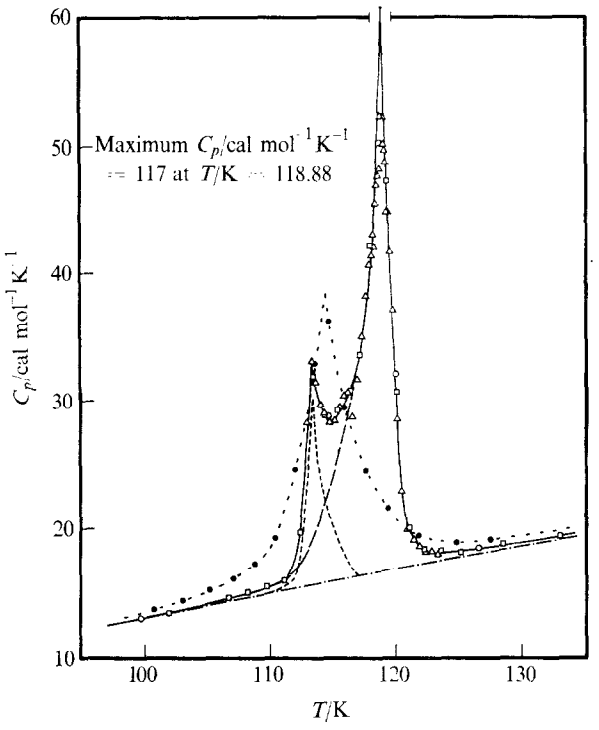

FIGURE 2. Heat capacity of magnetite in the transition region. ○ represents series I, □ represents series II, △ represents series III. – ● – ● – represents data by Millar,[2] –·–·– represents estimated lattice heat capacity, – – – represents resolution of lower temperature peak, — — — represents resolution of higher temperature peak.

nature of the transition. This was clearly demonstrated by the change in temperature dependence of the electrical conductivity[19] on synthetic samples with slightly different oxygen content. Characteristic changes in magneto-crystalline anisotropy[20] and acoustic-loss peaks[21] also result from small variations in oxygen content. Impurities have an equally detrimental effect on the transition as demonstrated by heat-capacity measurements on the natural magnetite crystal from Kiruna, Sweden, as well as by numerous studies reported in the literature. It is, however, considered unlikely that the double peak is due to impurities in the sample or to the fact that it was heated in a silica tube, since the spectrographic analysis showed the presence of less than 0.01 per cent metallic impurities (including silicon). Gross inhomogeneity (or phase separation) in the sample might account for the behavior. It is known[22] that the Fe_3O_4-phase has a considerable range of homogeneity, extending between the limits $FeO_{1.333}$ and $FeO_{1.382}$ at 1457°C. What happens to this solid solution on cooling under non-equilibrium conditions has not yet been studied in detail, but it is conceivable that phases with slightly different composition and structure might be formed, as in the VO_{2-x}[23] and TiO_{2-x}[24] systems. Until evidence confirming these or other explanations is available, the double maximum in the heat-capacity curve

is considered to be a property of Fe_3O_4. Other relevant information concerning the transition region will now be introduced. The discussions will be limited to some simple property changes. The large body of cross-related effects, i.e. thermoelectric, magneto-caloric, magneto-electric, etc., will not be considered.

STRUCTURAL ASPECTS

After the atomic coordinates in crystalline magnetite near 300 K had been refined by X-ray diffraction methods,[25] Verwey and De Boer[26] concluded that Fe_3O_4 has an inverse-spinel-type structure with Fe^{2+} and Fe^{3+} ions distributed at random over the octahedral positions. Subsequently, Verwey[19] inferred that the transition phenomenon involves an order–disorder effect on the ions at the octahedral positions. Below the transition temperature the ferrous and ferric ions form mutually perpendicular rows parallel to (001). The structure was assumed to have tetragonal symmetry[27] although orthorhombic symmetry[28] would be more appropriate. X-ray powder photographs of magnetite below the transition temperature were interpreted in terms of a rhombohedral unit cell,[10,29] while other authors[11,30] claimed that it was orthorhombic. Symmetry considerations[31] show that transition from the reported orthorhombic structure to the cubic one is possible only as a first-order transition and not as a higher-order transition.

No conclusion regarding the distribution of Fe^{2+} and Fe^{3+} ions among the tetrahedral and octahedral lattice sites could be drawn on the basis of X-ray data, but Néel[32] interpreted the magnetic data on magnetite by assuming antiferromagnetic coupling between the spin moments of the Fe^{3+} ions on A-sites and the Fe^{2+} and Fe^{3+} ions on B-sites. This antiferromagnetic arrangement was strongly supported by neutron diffraction work on magnetite powder by Shull *et al.*[33] Further neutron diffraction work by Hamilton[34] on synthetic crystals gave a convincing confirmation of the Verwey order scheme. Recent neutron diffraction work[35] has shown the presence of extra reflexions below the transition which are attributed to a doubling of the *c*-axis. In a natural crystal these reflections disappeared gradually between 100 and 120 K, while for a synthetic crystal they vanished abruptly at (118.5 ± 1) K. Thus, there are indications of complex structural behavior of magnetite in the transition region and of a continuous transition being precluded by symmetry conditions. The presence of an intermediate structure which can accommodate increasing disorder, therefore, seems plausible.

ELECTRICAL ASPECTS

The high electrical conductivity of magnetite was rationalized[36,37] in terms of random distribution of Fe^{2+} and Fe^{3+} ions over equivalent lattice positions. As the temperature is lowered a sudden decrease in conductivity is observed.[3,6,38] In stoichiometric synthetic single crystals the transition is reported[6] to take place at (119.4 ± 0.3) K, and it is marked by the conductivity dropping by a factor of 90 within a temperature interval of about 1 K. The conductivity is anisotropic below the transition, as also noted earlier.[27]

Hall effect and thermal e.m.f. measurements have led to the conclusion[39] that the electrical conductivity of stoichiometric Fe_3O_4 is of electronic origin. Theoretical

considerations[40] are in agreement with a hopping electron model above the transition, and a thermally-activated hopping mechanism involving a fairly complex defect below the transition.[41] The transition is considered[42] to be of the Mott-Wigner type in which the low-density insulating state is brought about by electron correlation. The pressure dependence of the conductivity[43] is consistent with such a model.

The temperature dependence of the electrical resistivity in magnetic fields was reported[44] and found to show two minima, one at 111.5 K and the other at 95 K, presumably due to the dispersion of electrons over fluctuations in magnetization and density, respectively.

Characteristic anomalies in the thermoelectric and Nernst-Ettingshausen effects in the low-temperature transition region were taken[45] to indicate a reorganization of the energy spectrum of the conductivity electrons in magnetite.

MAGNETIC ASPECTS

The magnetic properties of magnetite samples were measured by Weiss and Forrer[15] and the highest magnetization values found to be associated with the stoichiometric composition Fe_3O_4. At 120 K a transition was observed which, however, did not affect its magnetic moment (i.e., 4.07 Bohr magnetons per molecule of Fe_3O_4 extrapolated to 0 K). The small variation in electrical conductivity with magnetic field strength[46–48] is in keeping with the view that the spontaneous magnetization does not change during the transition. The low moment was explained by the Néel theory of ferrimagnetism[32] on the assumption that the magnetic moments of the Fe^{3+} ions are mutually annihilated by antiferromagnetic coupling. On the basis of magnetization,[49,50] thermal expansion, and magnetostriction[51] measurements, the possible origin of the magnetic anistropy below the transition is discussed.[52] Additional results from magnetostriction,[53] hysteresis loop and strain gauge measurements,[54,55] and magnetic torque curves[56–60] established the structure below the transition as orthorhombic, and magnetic anistropy constants were derived.

In contrast to the results of an earlier calculation,[61] Slonczewski[62] finds that the calculated anistropy constants ($K_a = -1.2\ \mathrm{J\ cm^{-3}}$, $K_b = 1.2\ \mathrm{J\ cm^{-3}}$) disagree with the experimental values ($K_a \approx 0.05\ \mathrm{J\ cm^{-3}}$, $K_b \approx 0.05\ \mathrm{J\ cm^{-3}}$) both with regard to order of magnitude and direction of easy magnetization. The presence of disorder might, however, account for the discrepancy.

Ferrimagnetic-resonance results[28,63,64] have been interpreted in terms of domain structures[65] and twinning[8,64] and separate contributions from the ferric ions at octahedral and tetrahedral sites.[66] The discrepancy between the g-factor obtained by this method and nuclear magnetic resonance studies[67,68] suggests that some unexplained effect obscures the ferrimagnetic resonance results.[69]

Mössbauer absorption spectra[70–73] differ in detail. They are interpreted in terms of electron hopping among the octahedral Fe^{2+} and Fe^{3+} ions at 300 K, which produces an averaged spectrum clearly distinguishable from that of the tetrahedral Fe^{3+} ions. At 77 K, where the hopping has ceased, the three kinds of ions should show their separable spectra, but no difference between the two types of Fe^{3+} ions could be observed. This can be understood[69] on the assumption that the hyperfine

field at the Fe^{3+} nucleus is the same on octahedral and tetrahedral sites—apart from the sublattice magnetization, which in this case is probably also equal—since the spin quantum numbers are the same ($S = 5/2$).

THERMODYNAMIC ASPECTS

The enthalpy and entropy increments associated with the transition were evaluated by subtracting the lattice contribution from the total increments in the range 100 to 140 K. The lattice heat-capacity values were estimated on the basis of a gradual change in Debye Θ's with temperature from $\Theta/K = 550$ at 100 K to 571 at 140 K (see figure 2). The results are given in table 3. The total entropy increment observed, 1.35 cal mol^{-1} K^{-1}, agrees well with the value 1.3 cal mol^{-1} K^{-1} estimated from Parks and Kelley's[1] results as $\Delta H/\Delta T$ for $T = 115$ K, and the value 1.05 cal mol^{-1} K^{-1} evaluated graphically from Millar's[2] results.

TABLE 3. Enthalpy and entropy of transition in magnetite[a]

Series		T_1/K	T_2/K	$H(T_2)-H(T_1)$ / cal mol^{-1}	$H(125\text{ K})-H(110\text{ K})$ / cal mol^{-1}
I	7–10	103.515	130.500	598.59	402.0
IV	130	109.884	124.245	388.51	400.4
V	131	110.023	124.847	397.46	400.5
VI	132	110.036	129.060	477.55	402.3
VII	133	110.081	125.113	401.95	401.2
VIII	134	109.758	124.959	404.71	401.7
			Mean value $H(125\text{ K})-H(110\text{ K})$		= 401.3
			−Lattice contribution $H(125\text{ K})-H(110\text{ K})$		= −246.3
					155
			+Excess below 110 K $\Delta\{H(110\text{ K})-H(100\text{ K})\}$		= 1
			+Excess above 125 K $\Delta\{H(140\text{ K})-H(125\text{ K})\}$		= 2
			Enthalpy of transition ΔH_t		= 158
			Entropy of transition $\Delta S_t = 1.35$ cal mol^{-1} K^{-1}		

[a] 1 cal = 4.184 J; 1 mol $Fe_3O_4 \triangleq 231.55$ g.

Resolution of the heat-capacity peaks into their components is rather difficult, and cannot be done by ascribing the same shape to both of them. In fact, the pre-transition effects associated with the higher-temperature peak appear to extend below the onset of the lower-temperature transition. The latter may involve a phase transition from the orthorhombic to an intermediate structure (with an entropy increment of only about 0.2 cal mol^{-1} K^{-1}), related to a change in crystal structure upon onset of long-range disorder of the Fe^{2+} and Fe^{3+} ion distribution.

As discussed by Anderson[74] the octahedral lattice sites in the spinel structure form an arrangement for which it is possible to achieve essentially perfect short-range order while maintaining a finite entropy. The sites can be described in terms of

tetrahedra arranged on a diamond lattice and connected at their apices. Each site is presumably occupied by one of two kinds of iron atoms present in equal numbers. We are concerned with changes in their distribution with temperature, and with residual disorder. Questions also arise with regard to the physical difference between the two kinds of atoms, and how they interconvert.

The available evidence indicates that the magnetic moment of magnetite does not change during the transition. Thus the characteristic difference between the atoms on the octahedral sites in this context is that half of them possess five unpaired 3d electrons and the other half four unpaired electrons and one unshared pair. The order–disorder process therefore involves distribution of $(N/2)$ localized 3d electrons over N atoms. The process by which this takes place has not been clarified in detail; it conceivably involves both valence and conduction electrons. Calculations of the coulombic order energy[75–78] in Fe_3O_4 yields 39.3 kcal mol^{-1} and indicates that considerable short-range order is present above the transition. Anderson[74] suggests that the short-range order might be discussed as one in which there is a maximum number of Fe^{2+}–Fe^{3+} pairs; i.e. two Fe^{2+} and two Fe^{3+} ions are present on each tetrahedron.

Assuming nearest-neighbor interactions only, one can find a number of configurations, all of which have the lowest possible energy. Long-range coulombic forces are only 5 per cent effective in creating long-range order. More recently a general expression for the correlation function was obtained.[79] Under simplified conditions the energy decrement between the Anderson short-range ordered and the Verwey structures was calculated to be only 3.8 per cent. Complete ordering might not be achieved, therefore, on cooling magnetite through the transition region.

The residual or zero-point entropy might be estimated in a manner similar to that employed by Pauling[80] for ice. The resulting lower limit for one mole of Fe_3O_4 is

$$S_0 = 0.81 \text{ cal mol}^{-1} \text{ K}^{-1}.$$

The expected entropy change from complete order to complete disorder is equal to $2R \ln 2$ per mole Fe_3O_4, i.e. 2.75 cal mol^{-1} K^{-1}, while the actually observed value is only 1.35 cal mol^{-1} K^{-1}. Some part of the difference is presumably due to residual entropy below the transition, and some to short-range order persisting above the transition. A different view on the transition is adopted by de Bergevin and Brunel.[81] They suggest that Slater's model[82] for the ferroelectric transition in potassium dihydrogenphosphate is applicable to the transition in magnetite and conclude that it involves change from complete long-range order to short-range order with an entropy increment

$$\Delta S_t = 0.78 \text{ cal mol}^{-1} \text{ K}^{-1}.$$

In the high-temperature limit the disorder entropy is reported to be 0.81 cal mol^{-1} K^{-1}. These entropy values are, however, only about half of that observed here and cast doubt upon the applicability of the model.

The possible existence of zero-point entropy in magnetite needs further verification from combination of thermal and equilibrium data for suitable reactions. One such reaction is

$$3\text{Fe(s)} + 4\text{H}_2\text{O(g)} = \text{Fe}_3\text{O}_4\text{(s)} + 4\text{H}_2\text{(g)},$$

for which equilibrium results exist and thermal results are precisely known except for the heat capacity of Fe_3O_4 above 350 K. Such measurements are in progress. Upon completion, the problem can then be reconsidered.

SPIN WAVE CONTRIBUTIONS

The effect of elementary excitations of the spin system of inverse spinels has been considered by Kouvel[83] and shown to occasion an $\alpha T^{3/2}$ contribution to the heat capacity at very low temperatures in addition to the Debye βT^3 lattice term. Heat-capacity measurements by Kouvel[5] in the range 1.2 to 4.2 K indicated a much higher spin-wave contribution than is consistent with theory. Results on iron-substituted nickel ferrites[84] ($Ni_xFe_{2+x}O_4$ with $x = 1.0$, 0.88, and 0.58) also indicate a high value for magnetite. Later measurements by Dixon *et al.*[7] over the same region are considerably lower, but not as low as required by theory. Our values over the 5 to 10 K region are plotted as $CT^{-3/2}$ *versus* $T^{3/2}$ in figure 3 together with the earlier results. They are in accord within experimental error with those by Dixon *et al.*[7]

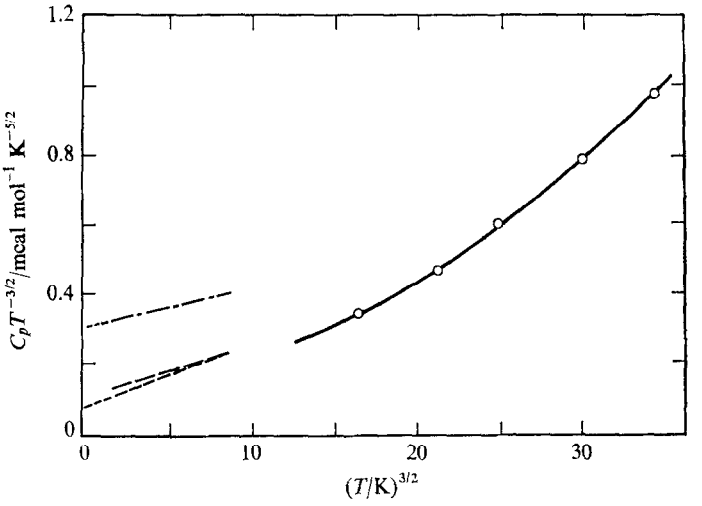

FIGURE 3. Spin-wave contributions to the heat capacity of magnetite. —○—○— represents experimental results on synthetic magnetite, and — — represents two series of results of Dixon *et al.*[7] —·—·— represents results of Kouvel.[5]

According to Kouvel[83] the spin-wave heat capacity in the absence of long-range order on the octahedral site is

$$C_m = 0.113\left\{\frac{(2S_B - S_A)kT}{-(11/2)J_{AB}S_AS_B + J_{AA}S_A^2 + 2J_{BB}S_B^2}\right\}^{3/2}$$

where S_A and S_B are the spin quantum numbers $S_A = 5/2$ and $S_B = (1/2)(5/2+4/2) = 9/4$, respectively; J_{AA}, J_{AB}, and J_{BB} are exchange integral values for the AA, AB, and BB interactions. According to Néel,[32] all the interchange interactions in ferrites are antiferromagnetic and $J_{AB} \gg J_{AA}$ or J_{BB} as a result of the relative magnitudes of the superexchange.

Spin-wave dispersion relations for magnetite have been derived[69,85–89] and dispersion curves obtained by inelastic neutron scattering techniques above the transition[90–93] and below.[94,95]

In the earlier work only J_{AB} was considered while the most recent evaluation[96] leads to $J_{AA} = (-1.52 \pm 0.46)$ meV, $J_{AB} = (-2.42 \pm 0.04)$ meV, and $J_{BB} = (0.31 \pm 0.07)$ meV. With these results the intercept on the ordinate of figure 3 should be 0.031 mcal mol^{-1} $K^{-5/2}$ assuming the absence of long-range order of the spins on the octahedral sites.

Kouvel has also provided expressions for the spin-wave heat capacity in the ordered state. As it has been observed that at least the J_{AB} and J_{BB} values are almost equal above and below the transition,[94,95] the above values were used in the evaluation which, however, gave the same intercept. Thus, spin-wave contributions of only 40 per cent of the lowest value by Dixon *et al.*[7] are accounted for by theory. A firm conclusion can be drawn only from measurements at lower temperatures than those reported here.

The continuing support of the Division of Research of the U.S. Atomic Energy Commission is gratefully acknowledged. We also wish to thank Norman E. Levitin for performing most of the heat-capacity measurements, Torkild Thurmann-Moe for assistance in synthesizing the calorimetric sample, and Clinton F. Jefferson for analytical and magnetic moment determinations.

REFERENCES

1. Parks, G. S.; Kelley, K. K. *J. Phys. Chem.* **1926,** 30, 47.
2. Millar, R. W. *J. Amer. Chem. Soc.* **1929,** 51, 215.
3. Okamura, T. *Sci. Repts. Tôhoku Imp. Univ. First Series* **1932,** 21, 231.
4. Okamura, T.; Torizuka, Y. *Sci. Repts. Res. Insts. Tôhoku Univ.* **1950,** *A2*, 352.
5. Kouvel, J. S. *Phys. Rev.* **1956,** 102, 1489.
6. Blythe, H.; Harvey, T. J.; Hoare, F. E.; Moody, D. E. *Cryogenics* **1964,** 4, 28.
7. Dixon, M.; Hoare, F. E.; Holden, T. M. *Phys. Letters* **1965,** 14, 184.
8. Calhoun, B. A. *Phys. Rev.* **1954,** 94, 1577.
9. Slack, G. A. *Phys. Rev.* **1962,** 126, 426.
10. Tombs, N. C.; Rooksby, H. P. *Acta Cryst.* **1951,** 4, 474.
11. Abrahams, S. C.; Calhoun, B. A. *Acta Cryst.* **1955,** 8, 257.
12. Basta, E. Z. *Mineral Mag.* **1957,** 31, 431.
13. Swanson, H. E.; McMurdie, H. F.; Morris, M. C.; Evans, E. H. Natl. Bur. Std. (U.S.) Monograph 25, Section 5, Standard X-ray Diffraction Patterns, Washington, D.C. **1967,** p. 31.
14. Gorter, E. W. *Compt. Rend.* **1950,** 230, 192; *Nature* **1950,** 165, 798; Thesis, Leiden **1954;** *Philips Res. Repts.* **1954,** 9, 295.
15. Weiss, P.; Forrer, R. *Ann. phys.* **1929,** [10] 12, 279.
16. Pauthenet, R. *Ann. phys.* **1952,** [12] 7, 710.
17. Westrum, E. F. Jr.; Furukawa, G. T.; McCullough, J. P. In *Experimental Thermodynamics,* Vol. 1. Editors: J. P. McCullough and D. W. Scott. Butterworths. London. **1968.** p. 333.
18. Coughlin, J. P.; King, E. C.; Bonnickson, K. R. *J. Amer. Chem. Soc.* **1951,** 73, 3891.
19. Verwey, E. J. W. *Nature* **1939,** 144, 327; *Chem. Weekblad* **1942,** 39, 30. See also Verwey, E. J. W. ; Haayman, P. W. *Physica* **1941,** 8, 979.
20. Sharma, V. N. *Phys. Letters* **1965,** 19, 462.
21. Suiter, W. B. Jr.; Blair, R. *J. Appl. Phys.* **1965,** 36, 1156.
22. Darken, L. S.; Gurry, R. W. *J. Amer. Chem. Soc.* **1946,** 68, 798.

23. Andersson, S.; Collén, B.; Kuylenstierna, U.; Magnéli, A. *Acta Chem. Scand.* **1957,** 11, 1647.
24. Andersson, S. *Acta Chem. Scand.* **1954,** 8, 1599.
25. Claasen, A. A. *Proc. Phys. Soc.* (*London*) **1926,** 38, 482; 39, 342.
26. Verwey, E. J. W.; De Boer, J. H. *Rec. trav. chim.* **1936,** 55, 531.
27. Verwey, E. J. W.; Haayman, P. W.; Romeijn, F. C. *J. Chem. Phys.* **1947,** 15, 181.
28. Bickford, L. R., Jr. *Phys. Rev.* **1949,** 75, 1298; 76, 137; **1950,** 78, 449.
29. Rooksby, H. P.; Willis, B. T. M. *Acta Cryst.* **1953,** 6, 565.
30. Abrahams, S. C.; Calhoun, B. A. *Acta Cryst.* **1953,** 6, 105.
31. Haas, C. *J. Phys. Chem. Solids* **1965,** 26, 1225.
32. Néel, L. *Ann. phys.* **1948,** [12] 3, 137.
33. Shull, C. G.; Wollan, E. O.; Strauser, W. A. *Phys. Rev.* **1951,** 81, 483; Shull, C. G. *Phys. Rev.* **1951,** 81, 626; Shull, C. G.; Wollan, E. O.; Koehler, W. C. *Phys. Rev.* **1951,** 84, 912.
34. Hamilton, W. C. *Phys. Rev.* **1958,** 110, 1050.
35. Samuelsen, E. J.; Bleeker, E. J.; Dobrzynski, L.; Riste, T. *J. Appl. Phys.* **1968,** 39, 1114. See also Kjeller Report KR-122, October **1967.**
36. Wagner, C.; Koch, E. *Z. Phys. Chem.* **1936,** B32, 439.
37. De Boer, J. H.; Verwey, E. J. W. *Proc. Phys. Soc.* (*London*) **1937,** 49, 59.
38. Miles, P. A.; Westphal, W. B.; von Hippel, A. *Rev. Mod. Phys.* **1957,** 29, 279.
39. Lavine, J. M. *Phys. Rev.* **1959,** 114, 482.
40. Haubenreisser, W. *Phys. Stat. Solidi* **1961,** 1, 619.
41. Tannhauser, D. S. *Phys. Kond. Materie* **1964,** 3, 146.
42. Adler, D. *Rev. Mod. Phys.* **1968,** 40, 714.
43. Samara, G. A. *Phys. Rev. Letters* **1968,** 21, 795.
44. Zotov, T. D. *Fiz. Metal i Metalloved., Akad. Nauk S.S.S.R.* **1960,** 9, 48; **1959,** 8, 639; **1959,** 7, 906.
45. Samokhvalov, A. A.; Fakidov, I. G. *Fiz. Metal i Metalloved., Akad. Nauk S.S.S.R.* **1960,** 9, 31; **1959,** 8, 694; **1959,** 7, 465. See also Davidenko, N. I.; Samokhvalov, A. A.; Fakidov, I. G. *Soviet Phys.-Solid State* **1961,** 3, 1197.
46. Shirakawa, Y. *Phys. Rev.* **1941,** 60, 835.
47. Watanabe, H.; Tsuya, N. *Sci. Repts. Res. Insts. Tôhoku Univ.* **1950,** A2, 29.
48. Okamura, T.; Torizuka, Y.; Kojima, H. *Sci. Repts. Res. Insts. Tôhoku Univ.* **1949,** A1, 479.
49. Li, C. H. *Phys. Rev.* **1932,** 40, 1002.
50. Okamura, T.; Ogawa, S. *Proc. Phys.-Math. Soc. Japan* **1941,** 23, 363; **1943,** 25, 43.
51. Domenicali, C. A. *Phys. Rev.* **1950,** 78, 458.
52. Watanabe, H. *Sci. Repts. Res. Insts. Tôhoku Univ.* **1950,** *A2,* 280.
53. Bickford, L. R., Jr. *Rev. Mod. Phys.* **1953,** 25, 75.
54. Stull, J. L.; Bickford, L. R., Jr. *Phys. Rev.* **1953,** 92, 845.
55. Bickford, L. R., Jr.; Pappis, J.; Stull, J. L. *Phys. Rev.* **1955,** 99, 1210.
56. Williams, H. J.; Bozorth, R. M. *Rev. Mod. Phys.* **1953,** 25, 79.
57. Williams, H. J.; Bozorth, R. M.; Goertz, M. *Phys. Rev.* **1953,** 91, 1107.
58. Narovskaya, N. P. *Izvest. Akad. Nauk S.S.S.R.* **1958,** Ser. Fiz. 22, 1200. See also *Kristallografiya* **1958,** 3, 346.
59. Palmer, W. *Phys. Rev.* **1963,** 131, 1057.
60. Pearson, R. F.; Cooper, R. W. *Proc. Phys. Soc.* (*London*) **1961,** 78, 17.
61. Yoshida, K.; Tachiki, M. *Progr. Theoret. Phys.* (*Kyoto*) **1957,** 17, 331.
62. Slonczewski, J. C. *J. Appl. Phys.* **1961,** 32, 2535.
63. Hirone, T.; Watanabe, H.; Mizuno, J.; Tsuya, N. *Sci. Repts. Res. Insts. Tôhoku Univ.* **1950,** *A2,* 774. See also Okamura, T.; Torizuka, Y. *Sci. Repts. Res. Insts. Tôhoku Univ.* **1950,** *A2,* 882; **1951,** *A3,* 214.
64. Bonstrom, D. B.; Morrish, A. H.; Watt, L. A. K. *J. Appl. Phys.* **1961,** 32, 2725.
65. Nagamiya, T. *Progr. Theoret. Phys.* (*Japan*) **1953,** 10, 72.
66. Bickford, L. R., Jr. *Phys. Rev.* **1953,** 92, 845.
67. Ogawa, S.; Morimoto, S. *J. Phys. Soc. Japan* **1962,** 17, 654. See also Ogawa, S.; Morimoto, S.; Kimura, Y. *J. Phys. Soc. Japan* **1962,** 17, 1671.
68. Boyd, E. L. *Phys. Rev.* **1963,** 129, 1961.
69. Callen, E. *Phys. Rev.* **1966,** 150, 367.
70. Solomon, I. *Compt. Rend.* **1960,** 251, 2675.
71. Bauminger, R.; Cohen, S. G.; Marinov, A.; Ofer, S.; Segal, E. *Phys. Rev.* **1961,** 122, 1447.
72. Ito, A.; Ôno, K.; Ishikawa, Y. *J. Phys. Soc. Japan* **1963,** 18, 1465. See also *J. Phys. Soc. Japan* **1962,** 17B, 125.

73. Banerjee, S. K.; O'Reilly, W.; Johnson, C. E. *J. Appl. Phys.* **1967,** 38, 1289.
74. Anderson, P. W. *Phys. Rev.* **1956,** 102, 1008.
75. Verwey, E. J. W.; Heilmann, E. L. *J. Chem. Phys.* **1947,** 15, 174.
76. Verwey, E. J. W.; De Boer, F.; Van Santen, J. H. *J. Chem. Phys.* **1948,** 16, 1091.
77. De Boer, F.; Van Santen, J. H.; Verwey, E. J. W. *J. Chem. Phys.* **1950,** 18, 1032.
78. Van Santen, J. H. *Philips Res. Rept.* **1950,** 5, 282.
79. Matsuura, T.; Yamada, K.; Yoshimori, A. *Prog. Theoret. Phys. (Japan)* **1966,** 36, 679.
80. Pauling, L. *The Nature of the Chemical Bond,* 3rd ed. Cornell University Press. Ithaca, N.Y. **1960.** p. 466.
81. de Bergevin, F.; Brunel, M. *Compt. Rend.* **1968,** 266B, 88.
82. Slater, J. C. *J. Chem. Phys.* **1941,** 9, 16.
83. Kouvel, J. S. Tech. Rept. 210, Cruft Laboratory, Harvard University, Cambridge, Mass. **1955.**
84. Pollack, S. R.; Atkins, K. R. *Phys. Rev.* **1962,** 125, 1248.
85. Kaplan, H. *Phys. Rev.* **1952,** 86, 121.
86. Milford, F. J.; Glasser, M. L. *Phys. Letters* **1962,** 2, 248.
87. Glasser, M. L.; Milford, F. J. *Phys. Rev.* **1963,** 130, 1783.
88. Kenan, R. P.; Glasser, M. L.; Milford, F. J. *Phys. Rev.* **1963,** 132, 47.
89. Mills, R. E.; Kenan, R. P.; Milford, F. J. *Phys. Rev.* **1966,** 145, 704.
90. Riste, T.; Blinowski, K.; Janik, J. *J. Phys. Chem. Solids* **1959,** 9, 153.
91. Watanabe, H.; Brockhouse, B. N. *Phys. Letters* **1962,** 2, 248, 1892. See also IAEA Symposium, Inelastic Scattering of Neutrons in Solids and Liquids. IAEA. Vienna. **1963,** p. 297 and *Phys. Letters* **1962,** 1, 189.
92. Ferguson, G. A., Jr.; Saenz, A. W. *Phys. Rev.* **1967,** 156, 632.
93. Dimitrijevic, Z.; Krasnicki, S.; Todviovic, J.; Wanic, A. *Phys. Stat. Solidi* **1967,** 22, 155. See also *Phys. Stat. Solidi* **1966,** 15, 119.
94. Alperin, H. A.; Steinsvoll, O.; Nathans, R.; Shirane, G. *Phys. Rev.* **1967,** 154, 508.
95. Torrie, B. H. *Sol. State Comm.* **1967,** 5, 715.
96. Möglestue, K. T. IAEA Symposium on Neutron Inelastic Scattering, Copenhagen, 20–25 May **1968,** SM-104/63.